JOURNAL OF APPLIED ELECTROCHEMISTRY 8 (1978) 5–10

Hydrodynamic and mass transport phenomena in a multiple-electrode magnetoelectrolytic cell

S. MOHANTA*, T. Z. FAHIDY

Department of Chemical Engineering, University of Waterloo, Canada

Received 14 January 1977

The effect of imposing a uniform magnetic field on an electrolytic cell with multiple parallel-plate electrodes is analysed in terms of hydrodynamic and mass transport phenomena with particular regard to cell design in the laminar flow regime.

List of Symbols

a electrode length
B magnetic flux density
b electrode separation distance
d electrode height
d_e equivalent diameter $= 4bd/(b + 2d)$
F MHD body force density $= JB$
f_c liquid head loss factor in curvature
g acceleration due to gravity
h_c liquid head loss due to curvature
h_f liquid head loss due to friction
h_M liquid head generated by the MHD body force
J magnitude of current density
(Pe) Peclet number $= (Re)(Sc)$
r_c curvature of the path of the floating particle on the electrolyte surface
(Ra) Rayleigh number $= (Sc)(Gr)$ [(Gr): Grashof number]
(Re) Reynolds number
S slope of an open-flow channel
(Sc) Schmidt number
(Sh) Sherwood number, based on the electrode height as characteristic length
T_p time required for the completion of a vortex motion about the electrode for a floating particle
$\bar{V}$ average electrolyte velocity
$\bar{V}_s$ average surface velocity in electrolyte
γ aspect ratio $= b/d$
μ dynamic viscosity of electrolyte
ν kinematic viscosity of electrolyte
ρ density of electrolyte

Abbreviations
CVD cell voltage drop
MHD magnetohydrodynamic

1. Introduction

The effect of a magnetic field on the behaviour of single-electrode pair-type electrochemical cells in d.c. electrolysis has been the subject of detailed investigation [1–3] and the enhancing influence of the magnetic field on cell performance has been analysed in terms of hydrodynamic [4, 5] and mass transfer [6–9] concepts. The augmentation of mass transport rates by the superposition of a magnetic field on a d.c. electric field in electrolysis has thus been demonstrated to be the result of increased and magnetohydrodynamically supported convective diffusion.

While single-electrode pair experiments have been useful for understanding the fundamental phenomena in magnetoelectrolysis, the beneficial effect of coupled electric/magnetic fields is more manifest in multiple-electrode cells where enhancement in mass transport can be much larger relative to the former. Since multiple-electrode cell configurations are of practical importance in certain electrochemical industries (e.g. electrorefining and electrowinning of metals), potentially useful benefits may be expected from magnetoelectrolytic multiple-electrode cell experiments upon appropriate scale-up to industrial cell size. The purpose of this paper is to describe such bench-scale experimental observations and to offer a hydrodynamics- and transport phenomena-based

* Present address: HSA Reactors Ltd., Rexdale, Ontario, Canada.

analysis bearing possible technological applications in mind.

2. Experimental

The experimental cell was made of Plexiglass and of size 15·2 cm x 5·1 cm x 5·1 cm. The cathodes and anodes (INCO copper refinery cathode sheets, 3·81 cm wide, active height: 3·34–4·1 cm) were placed alternatively in the cell and connected to their respective brass bus bars. In some experiments, the cell contained 5 anodes and 6 cathodes and, in some others, 6 anodes and 5 cathodes, by a proper interchange of the electrical connections. The electrodes were 0·795 mm thick at start and were separated by a distance of 1·19 cm. There was a 6·35 mm space between the edge of any electrode and the adjacent cell wall; the $CuSO_4$/H_2SO_4 electrolyte level varied slightly in different experiments. The apparatus for generating the magnetic field and d.c. electrolysis, the measuring and analytical techniques have previously been described [1–3].

The CVD/current density data were obtained via galvanostatic experiments where at a set current flow, steady-state CVD values were noted at different magnetic field strengths. At higher current and magnetic flux densities the CVD was found to fluctuate continuously due to excessive turbulence and in such cases an average of the oscillations was taken as a 'steady-state' value.

The pattern of the electrolyte surface motion was determined by measuring the time required for insoluble light particles (e.g. fish food) placed on the surface to complete a full vortex around an electrode: usually 3 or 4 readings per current flow and magnetic strength setting were adequate for computing its average value. Current efficiency tests were also carried out by finding the weight difference of the cathodes before and after electrolysis at a set current flow, magnetic field strength and time upon proper handling [1] of the fresh electrode surfaces: the value of the cathode current efficiency varied systematically between 97% and 99%.

The experimental observations are summarized in Tables 1–3 and Fig. 1; the latter shows the interrelation between the direction of current path

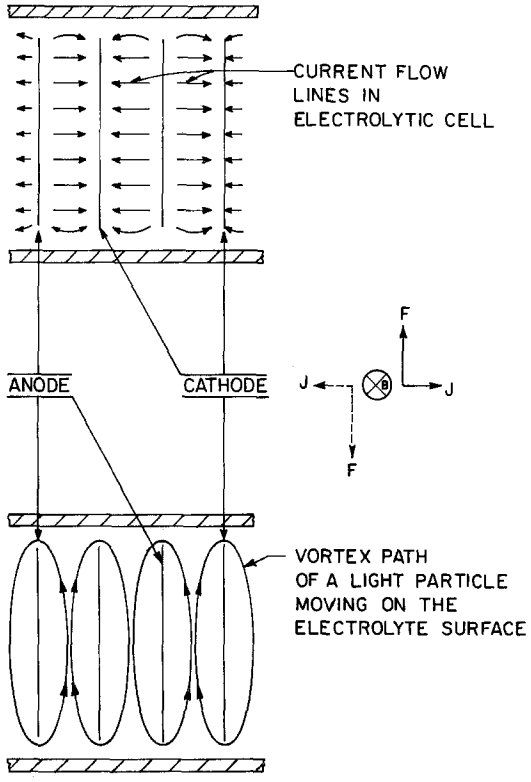

Fig. 1. Direction of current path, observed velocity pattern and MHD body force density in the experimental copper electrolysis cell.

Table 1. Characteristics of selected experimental conditions

	Electrolyte concentration (*mol dm*$^{-3}$)		*Electrode characteristics*		
Run no.	*$CuSO_4$*	*H_2SO_4*	*Active height* (*cm*)	*Total effective cathode area* (m^2)	*Temperature* (K)
MR05	0·048	1·560	4·10	0·0156	297·0
MR18	0·181	1·535	3·34	0·0127	294·4
MR41	0·409	1·570	3·97	0·0151	296·0

MR05, MR18: 6 cathodes, 5 anodes.
MR41: 6 anodes, 5 cathodes.

Table 2. Typical current density/cell voltage drop behaviour in transverse electric and magnetic fields, in the high current density region. [cell characteristics as in Table 1]

	MR05		*MR18*		*MR41*	
B (T)	*i* (Am^{-2})	*CVD* (V)	*i* (Am^{-2})	*CVD* (V)	*i* (Am^{-2})	*CVD* (V)
0·004*	30·30	0·505	133·1	0·598	309·82	0·460
	31·30	0·650	134·4	0·635	310·13	0·465
	32·42	0·710	134·9	0·664	312·70	0·472
0·110	40·80	0·315	179·5	0·555	676·00	0·350
	43·50	0·420	182·5	0·565	760·00	0·387
	71·90	0·620	185·8	0·575	923·00	0·410
0·540	136·30	0·400	198·6	0·510	676·00	0·309
	209·20	0·580	211·6	0·547	789·00	0·338
			224·0	0·573	956·00	0·361
0·785	135·90	0·370	211·6	0·537	677·00	0·307
	209·20	0·540	224·0	0·563	803·00	0·315
			236·0	0·590	958·00	0·358

* Residual flux density in 'turned-off' magnet position.

Table 3. Surface velocity data

	Current density, J ($A\,m^{-2}$)	*Magnetic field, B* (T)	*MHD body force density, F* ($N\,m^{-3}$)	*Time, T_p* (s)	$V \times 10^2$ $m\,s^{-1}$
Run MR05	36·0	0·055	1·98	17·125	0·561
	36·0	0·110	3·96	10·100	0·951
	36·0	0·200	7·20	4·725	2·034
	36·0	0·374	13·46	3·150	3·050
	36·0	0·540	19·44	2·870	3·350
	46·2	0·785	36·27	2·400	4·020
	46·2	0·540	24·95	3·050	3·150
	46·2	0·374	12·28	3·750	2·570
	46·2	0·200	9·24	5·350	1·762
	38·4	0·110	4·22	9·150	1·050
	63·5	0·110	6·99	8·800	1·092
	63·5	0·200	12·70	5·530	1·740
	63·5	0·374	23·75	3·230	2·980
	63·5	0·540	34·29	2·400	4·010
	63·5	0·785	49·85	2·000	4·800
	76·4	0·200	15·28	3·800	2·530
	76·4	0·374	28·57	3·100	3·100
	76·4	0·540	41·26	1·800	5·340
	76·4	0·785	59·97	1·300	7·400
Run MR41	23·4	0·785	18·37	3·000	3·170
	70·9	0·785	55·66	1·930	4·980
	119·8	0·055	6·59	4·400	2·183
	122·3	0·110	13·45	2·700	3·560
	122·3	0·200	24·46	2·600	3·690
	122·3	0·374	45·74	2·600	3·690
	186·1	0·055	10·24	3·800	2·555
	303·6	0·004	1·21	38·600	0·249
	349·9	0·030	10·50	5·300	1·816
	378·6	0·053	20·10	3·300	2·880

in the cell, the directions of surface motion and the related MHD body force density. The entire *i*/CVD behaviour for runs MR05 and MR18 has previously been presented [4]. The results indicate that the large enhancement in mass transport rates occurs even at relatively low magnetic flux densities. The higher the reactant ion concentration, the lower the relatively 'optimal' magnetic field strength; indeed, at $[Cu^{2+}] \cong 0{\cdot}41$ mol dm^{-3}, there seems to be little advantage to employing a magnetic field higher than about 0·110 T, whereas at $[Cu^{2+}] = 0{\cdot}05$ mol dm^{-3}, 0·54 T appears to be the optimal magnetic flux density. This rather important finding suggests that at industrially common electrolyte concentrations, relatively weak magnetic fields would have to be generated only at relatively small installation costs.

3. Analysis of the cell hydrodynamics

In a recent analysis of the hydrodynamic behaviour of single-electrode pair cells, the theory of open-channel hydraulics was employed in describing cell behaviour [5, 10]. In terms of the theory of hydraulics, one can state that the MHD body force creates a hydraulic head along the flow streamlines which is then balanced by head losses due to friction and curvature effects:

$$h_M = 2(h_f + h_c) = \frac{JB}{\rho g} a. \qquad (1)$$

Other loss components are ignored on the basis of order of magnitude arguments. A theoretical development which follows closely classical open-channel flow theory [10–12] leads to the following estimation formula of the surface vortex velocity:

$$\bar{V}_s = (1 - 1/2^4)Z(4)\frac{8b^2}{\pi^4}\frac{gS}{\nu} \qquad (2)$$

where $Z(4)$ is a Riemann's zeta-function and its numerical value is 1·082 32. On the other hand, the experimental value of this velocity may be computed (see Fig. 2) as

$$V_{obs} = \frac{2a + 2\pi r_c}{T_p}. \qquad (3)$$

Furthermore, the MHD body force density is related to the average electrolyte velocity as [1]

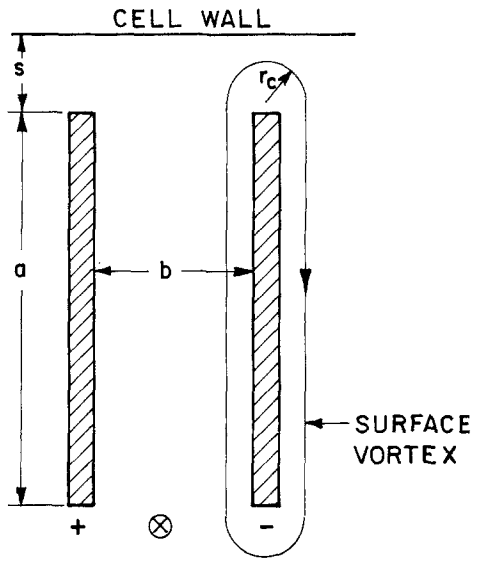

Fig. 2. Relationship between r_c, electrode separation b and electrode edge–cell wall separation, s. For the experimental case of $s \cong b/2$, $r_c = 1/2(s/2 + b/4)$. The vortex around the anode is not shown.

$$F = \frac{f_c}{2}\frac{\rho \bar{V}^2}{a} + \frac{12\mu}{b^2}\frac{\bar{V}}{(1 - 0{\cdot}314\gamma)}. \qquad (4)$$

Since, by theory [1],

$$\frac{\bar{V}_s}{\bar{V}} \cong \frac{1}{1 - 0{\cdot}314\gamma}$$

Equation 4 can further be written as

$$F = f_c\frac{\rho(1 - 0{\cdot}314\gamma)^2}{2a}\bar{V}_s^2 + \frac{12\mu}{b^2}\bar{V}_s. \qquad (5)$$

Equation 5 is the equation of a parametric family of curves where f_c is the *a priori* indeterminate parameter.

In Fig. 3 experimentally observed surface velocities were plotted against experimental MHD force densities, together with Equation 5: the lower solid line corresponds to the theoretical [11, 12] value of $f_c = 1{\cdot}4$ and the upper line has been obtained by statistical regression analysis, which corresponds to the somewhat smaller value of $f_c = 1{\cdot}1$. The above development being limited to the laminar flow regime, Equation 5 applies to surface vortex velocities less than about 0·5 m s^{-1} for this experimental apparatus, which is well above the observed velocities (see Table 3; no measurements were made in the turbulent zone

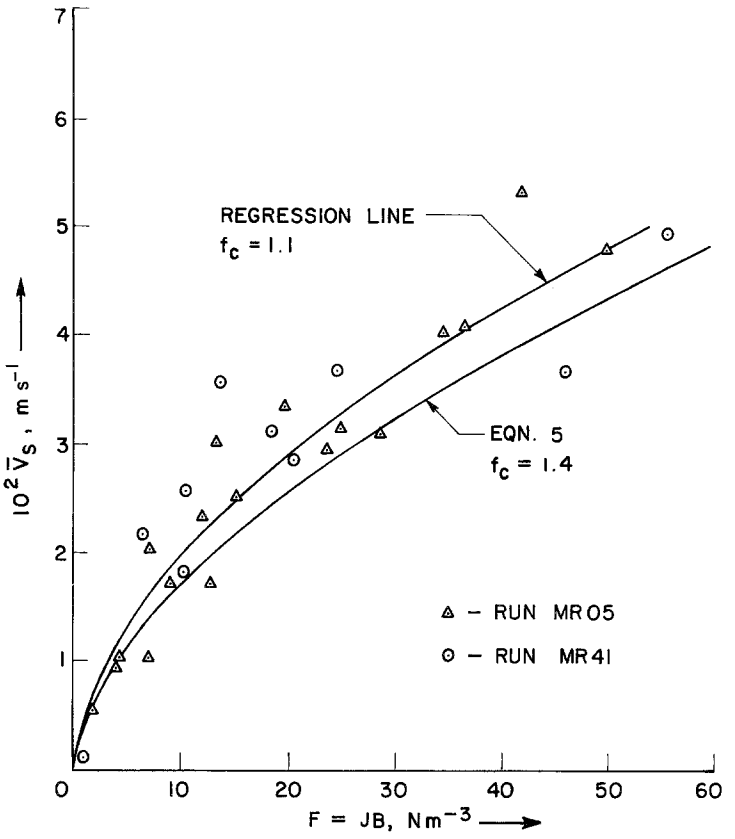

Fig. 3. The effect of the MHD body force density on the electrolyte surface velocity.

in as much as the movement of the floating particles could not be measured with sufficient accuracy).

4. Analysis of the mass transport aspects

A rigorous quantitative analysis of the mass transport phenomena is hindered by the absence of limiting current conditions at even weak magnetic fields in a multiple-electrode cell. While current densities at constant concentration polarization can, under certain circumstances, be estimated by a trial-and-error procedure in single-electrode pair cells [8], this procedure is not reliable in multiple-electrode cells where the forced convection component of the combined free and forced convection may cause uneven concentration distributions at different electrodes. A further complication is caused by a somewhat uneven current distribution at the electrodes; in the experimental cell, for example, the terminal cathodes were found to have usually gained 10% more weight than the inner cathodes, in a typical experimental run. In the absence of a magnetic field (i.e. in the residual field of 4 mT flux density) the well-known dimensionless mass transfer relationship [13]

$$(Sh) = 0{\cdot}67(Ra)^{0.25} \tag{6}$$

predicts $(Sh) = 192{\cdot}11$, $221{\cdot}14$ and $292{\cdot}77$ in runs MR05, MR18 and MR41, respectively, while the experimental values, upon correcting for current distribution effects, are $197{\cdot}39$, $215{\cdot}04$ and $287{\cdot}02$. One may conclude, therefore, that in the residual field, limiting current density conditions represent essentially free-convective diffusion control. In the case of stronger magnetic fields, the success of open-channel hydraulics theory in the analysis of cell hydrodynamics suggests that the mass transfer relationship [10]

$$(Sh) = 1{\cdot}85[(Pe)de/L]^{1/3} f(\gamma) \tag{7a}$$

$$f(\gamma) = \left(\frac{1-0{\cdot}271\gamma}{1-0{\cdot}314\gamma} \cdot \frac{1}{1+0{\cdot}5\gamma}\right)^{1/3} \tag{7b}$$

might be applied by proper extension of single electrode-pair conditions. Here the difficulty lies in the proper estimation of an apparent Reynolds (hence Peclet) number whose success is tied to the associated entry-region length for fully developed flow in an equivalent flow cell. In an approximate manner, one could estimate average electrolyte velocities, generated by the magnetically induced turbulence, via Fig. 2 at known values of i and B, and then estimate the apparent Reynolds number as

$$(Re) = \bar{V}d_e/\nu \qquad (8)$$

for insertion in Equation 7. A rigorous analysis would be hindered by two major difficulties: incompletely developed flow in the entry region (electrodes being in the entry region); the contribution of free and forced convection simultaneously to mass transfer phenomena at high ionic concentrations. Because of these combined effects the experimentally obtained (Sh) values are usually higher at the imposed magnetic flux densities than values predicted via Equation 7.

5. Concluding remarks

From an applied point of view, electrolysis in multiple-electrode cells and in transverse electric/magnetic fields is characterized by large current flow rates and good quality electrode deposits. In the current experiments with copper sulphate–sulphuric acid electrolytes, cathodic current densities ranging to 1200 A m^{-2} were observed at room temperature, and without H_2 evolution at the cathodes. This is about 3–4 times the advisable limit for current densities in industrial copper electrorefining practice at high temperatures; in all instances the copper deposit was found to be bright and firm.

A thorough analysis of the advantages of magnetic field super-position would have to weigh the incremental market value of the (cathode) product against installation and operating costs of the magnet, electric energy costs and other factors, as shown in a recent publication [14]; it is beyond the scope of this paper to offer a detailed economic analysis of the magnetoelectrolytic process described.

Given our present understanding of magnetohydrodynamic and transport phenomena in aqueous electrolyte systems, Equations 5 and 7 may be used as approximate design equations for multiple-electrode magnetoelectrolytic cells. Further studies would be required on a larger (preferably small or medium pilot plant) scale in order to explore concrete technological possibilities.

Acknowledgement

This project was supported by a National Research Council of Canada research grant and graduate scholarship.

References

[1] S. Mohanta, Ph.D. Thesis, Univ. of Waterloo (1974).
[2] S. Mohanta and T. Z. Fahidy, *Canad. J. Chem. Eng.* **50** (1972) 248.
[3] *Idem, ibid* **50** (1972) 434.
[4] T. Z. Fahidy, *Electrochim. Acta* **18** (1973) 607.
[5] S. Mohanta and T. Z. Fahidy, *J. Appl. Electrochim.* **6** (1976) 211.
[6] *Idem, Electrochim. Acta* **19** (1974) 835.
[7] *Idem, ibid* **19** (1974) 771.
[8] *Idem, ibid* **21** (1976) 149.
[9] T. Z. Fahidy, *Chem. Eng. J.* 7 (1974) 21.
[10] S. Mohanta and T. Z. Fahidy, *Electrochim. Acta* **21** (1976) 143.
[11] W. M. Owen, *Trans. Amer. Soc. Civil Engrs* **119** (1954) 1157.
[12] S. Timoshenko, "The Theory of Elasticity', McGraw Hill, New York (1934).
[13] J. S. Newman, 'Electrochemical Systems', Prentice-Hall, New York (1973).
[14] T. Z. Fahidy, *Chem. Eng. J.* **12** (1976) 23.